FIBER AND RESIN FLOW EVALUATION OF SHORT CARBON FIBER-REINFORCED COMPOSITES USING MOVING PARTICLE SEMI-IMPLICIT PARTICLE-SIMULATION METHOD

Mahiro Teratani, Kazutaka Mukoyama, Shuhei Matsuzawa
Kenta Mitsufuji, Fumikazu Miyasaka, Koushu Hanaki, Tetsusei Kurashiki

Graduate School of Engineering, Osaka University, Osaka, Japan
*corresponding author: *teratani-m15@mit.eng.osaka-u.ac.jp*

Keywords: Short fibers, Resin flowage, CFRP, Numerical analysis, Press forming

Abstract
Fiber-reinforced plastics (FRP) are expected to apply automobile parts to reduce their weight. Press forming of short fiber-reinforced composites using thermoplastics enables to mass produce FRP parts for automobile. Since short fiber placement and temperature of material have effects on mechanical property of FRP, evaluating flowability of resin and fibers temperature distribution during press forming is important. However, it is inefficient in terms of time and cost to optimize many designable parameters; temperature of mold, pressure, volume fraction of fiber, matrix properties, etc. based on experimental procedure. Therefore, flowability of resin and fibers during press forming and distribution of temperature in short fiber-reinforced composites were evaluated using Moving Particle Semi-implicit (MPS) method. It was suggested that the proposed numerical method was applicable to simulating press forming process of short fiber-reinforced composites.

1. Introduction

Since FRP have advantages in excellent specific strength and rigidity, FRP have been applied to transportation equipment such as aircrafts. Approximately 64 % of oil consumption in the world is for transportation, especially energy consumption for automobile has the majority [1]. For that reason applying FRP to automobile to reduce their weight is recently expected from the viewpoint of energy saving.

There is a problem of forming cycle time to manufacture FRP for automobile. Press forming short fiber-reinforced composites using thermoplastics enables to mass production of FRP for automobile which is applied to the complex-shaped portion. However, it is important to evaluate flowability of fibers and distribution of temperature of material, because the short fiber flows during press forming, and fiber placement and the distribution of temperature of material have effects on mechanical property of FRP [2]. Since experimental estimation is inefficient in terms of time and cost, MPS particle-simulation is used as numerical analysis method in this study. This method is efficient compared with finite element method when considering large deformation. Therefore, in this study, flowability of resin and fibers during press forming of short fiber-reinforced composites is evaluated by using MPS method.

Excerpt from ISBN 978-3-00-053387-7

2. Numerical approach for incompressible flow

2.1. Moving particle semi-implicit (mps) method

A continuum is assumed to be represented by a set of particles, and governing equations are discretized by particle interaction models that correspond to differential operators in the MPS method. A particle nearer to particle *i* is considered to have a greater influence on particle *i*, and the magnitude of the interaction at a distance *r* from particle *i* is represented by the following weight function *w*.

$$\omega(\mathrm{r}) = \begin{cases} \dfrac{r_e}{r} - 1. & (0 \leqq r \leqq r_e). \\ 0 & (r > r_e). \end{cases} \quad (1)$$

Within radius r_e from particle *i*, the effects of particles are considered. The sum of weight functions, called the particle number density (PND) *n*, is defined as follows.

$$n_i = \sum_{i \neq j} \omega\left(\left|\mathbf{r_j} - \mathbf{r_i}\right|\right) \quad . \quad (2)$$

PND is proportional to the density of the fluid. Since the density of the fluid is constant for incompressible flow, PND should take a constant value n^0.

The gradient model, divergence model and laplacian model by using particle interaction models are represented as Eq. (3) to Eq. (5).

$$\left\langle \nabla \phi \right\rangle_i = \frac{d}{n^0} \sum_{j \neq i} \left[\frac{\phi_j - \phi_i}{\left|\mathbf{r_j} - \mathbf{r}_i\right|^2} \left(\mathbf{r_j} - \mathbf{r}_i\right) \omega\left(\left|\mathbf{r_j} - \mathbf{r}_i\right|\right) \right]. \quad (3)$$

$$\left\langle \nabla \cdot \mathbf{\Phi} \right\rangle_i = \frac{d}{n^0} \sum_{j \neq i} \left[\frac{\mathbf{\Phi_{ij}} \cdot \left(\mathbf{r_j} - \mathbf{r_i}\right)}{\left|\mathbf{r_j} - \mathbf{r}_i\right|^2} \omega\left(\left|\mathbf{r_j} - \mathbf{r}_i\right|\right) \right] \quad (4)$$

$$\left\langle \nabla^2 \phi \right\rangle_i = \frac{2d}{\lambda n^0} \sum_{j \neq i} \left[\left(\phi_j - \phi_i\right) \omega\left(\left|\mathbf{r_j} - \mathbf{r}_i\right|\right) \right] .$$

$$\lambda = \frac{\sum_{j \neq i} \left[\left|\mathbf{r_j} - \mathbf{r}_i\right|^2 \omega\left(\left|\mathbf{r_j} - \mathbf{r}_i\right|\right) \right]}{\sum_{j \neq i} \omega\left(\left|\mathbf{r_j} - \mathbf{r}_i\right|\right)} . \quad (5)$$

Φ is a scalar variable, $\mathbf{\Phi}$ is a vector variable, *d* is the dimension number and the bracket < > indicates the operator based on the particle interaction model.

2.2. Calculation algorithm

The governing equations for incompressible flow are the conservation of mass and the Navier-Stokes equation. ρ is the density, *t* is time, **u** is the velocity, *P* is the pressure, ν is kinetic viscosity, **g** is gravity acceleration.

$$\frac{D\rho}{Dt} = 0 \quad . \quad (7)$$

$$\frac{D\mathbf{u}}{Dt} = -\frac{1}{\rho} \nabla P + \nu \nabla^2 \mathbf{u} + \mathbf{g} \quad . \quad (8)$$

When the position **r**, velocity **u** and pressure *P* of all particles are known at time *k*, the following algorithm is applied to calculate physical quantities at new time step *k*+1.

1. Calculation condition and initial position of particles are input.
2. Temporary values for the velocity and position are explicitly calculated from gravity term and viscous term of Eq. (8), as Eq. (9) and (10).

Excerpt from ISBN 978-3-00-053387-7

$$\mathbf{u}^* = \mathbf{u}^k + \Delta t\left[\nu\nabla^2\mathbf{u} + \mathbf{g}\right]^k . \tag{9}$$

$$\mathbf{r}^* = \mathbf{r}^k + \Delta t\mathbf{u}^* . \tag{10}$$

3. The pressure is calculated from Poisson's equation on pressure, as Eq. (11).

$$\nabla^2 P^{k+1} = -\frac{\rho_0}{\Delta t^2}\frac{n^* - n^0}{n^0} . \tag{11}$$

4. The position and velocity are adjusted by calculating pressure gradient term of Eq. (8), as Eq. (12)

$$\mathbf{u}' = -\frac{\rho_0}{\Delta t^2}\frac{n^* - n^0}{n^0} .$$

$$\mathbf{u}^{k+1}{}_\mathbf{i} = \mathbf{u}_\mathbf{i}^* + \mathbf{u}' . \tag{12}$$

$$\mathbf{r}_\mathbf{i}^{\mathbf{k+1}} = \mathbf{r}^* + \Delta t\mathbf{u}' .$$

2.3. Modeling of fiber

Fiber is modeled as a rigid body, and the flowability of fiber is calculated as the following algorithm. First, the position and velocity of fiber particles are calculated in the same procedure as fluid particles. Then, the position and velocity of fiber particles are adjusted. The position of the center of gravity $\mathbf{r_g}$ and the amount of movement of the center of gravity $\mathbf{r_g}'$ is calculated as Eq. (13) and (14). And the moment of inertia, *I*, of a rigid body consisting of *N* particles are calculated as Eq. (15). m is mass.

$$\mathbf{r}_\mathbf{g} = \frac{1}{N}\sum_{i=1}^{N}\mathbf{r}_\mathbf{i} . \tag{13}$$

$$\mathbf{r}_\mathbf{g}' = \frac{1}{N}\sum_{i=1}^{N}\left(\hat{\mathbf{r}}^{\mathbf{k+1}}{}_\mathbf{i} - \mathbf{r}^{\mathbf{k}}{}_\mathbf{i}\right) . \tag{14}$$

$$I = \sum_{i=1}^{N} m\left|\mathbf{r}_\mathbf{i} - \mathbf{r}_\mathbf{g}\right|^2 . \tag{15}$$

Second, the rotation of rigid body is calculated from the amount of angular momentum of all fiber particles, as Eq. (16).

$$\theta' = \frac{1}{I}\sum_{i=1}^{N} m\left(\mathbf{r}^{\mathbf{k}}{}_\mathbf{i} - \mathbf{r}^{\mathbf{k}}{}_\mathbf{g}\right)\times\left(\hat{\mathbf{r}}^{\mathbf{k+1}}{}_\mathbf{i} - \mathbf{r}^{\mathbf{k}}{}_\mathbf{i}\right) . \tag{16}$$

Finally, the position and velocity of fiber particles are collected to maintain a rigid shape. [3][4]

$$\mathbf{r}_\mathbf{i}' = \mathbf{r}_\mathbf{g}' + \begin{bmatrix}\cos\theta' & -\sin\theta' \\ \sin\theta' & \cos\theta'\end{bmatrix}\left(\mathbf{r}^{\mathbf{k}}{}_\mathbf{i} - \mathbf{r}^{\mathbf{k}}{}_\mathbf{g}\right) - \left(\mathbf{r}^{\mathbf{k}}{}_\mathbf{i} - \mathbf{r}^{\mathbf{k}}{}_\mathbf{g}\right) . \tag{17}$$

2.4. Numerical approach for highly viscous fluid

When calculating viscosity term of Eq. (8), numerical stability conditions of the number of spreading must be satisfied in the MPS method as Eq. (18). Since thermoplastic resin is high viscosity (i.e. 1.0 to 10^3 Pa·s), the time step size Δt is set very small and it requires enormous analysis time. Therefore, it is possible to reduce analysis time by changing the calculation of viscosity term of Eq. (8)from explicit method to implicit method as Eq. (19). [5][6]

$$\Delta t \le d_i\frac{\rho l^2}{\eta} . \tag{18}$$

$$\mathbf{u}_i^{**} = \mathbf{u}_i^{\,k} + \Delta t\left(\frac{2d\nu}{\lambda n^0}\sum_{j\neq i}\left(u_j^{**} - u_i^{**}\right)\omega\left(r_{ij}\right) + \mathbf{g}\right) . \tag{19}$$

l is the initial distance between particles, d_i is diffusion number ,d is dimension number.

Excerpt from ISBN 978-3-00-053387-7

3. Analysis of CFRP press forming

3.1. Evaluation of the effect of fibers on resin flow

The effects of fibers in resin flow is evaluated by comparing only resin model (Case 1) with resin and 5 fibers model (Case 2). Analysis model is shown in Fig. 1. The model consists of iron plates, carbon fibers and polypropylene. The density of polypropylene, carbon fibers, iron plate is 1000, 1600, 7800 kg/m^3,respectively. The viscosity of resin is 1.0 Pa· s. Analysis condition is summerized in Table 1. The particle size is 2mm, fiber length is 16mm, the width of resin is 60mm and the height of resin is 50mm. Time step is 1.0×10^{-5} s and the gravity is also considered as an external force.

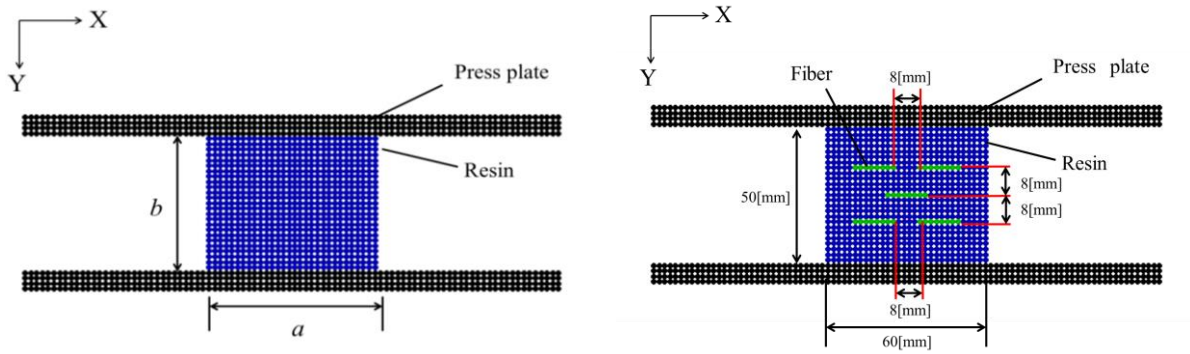

(a) Case 1 (b) Case 2

Fig. 1 Evaluation model of the effects of fiber on flowage.

Table 1. parameter of 5 fibers and resin model.

Press acceleration α_p	12.0 [m/s^2]
Gravity acceleration g	9.8 [m/s^2]
Resin viscosity μ	1.0 [Pa· s]
Time step Δt	1.0×10^{-5} [s]

The time history of pressure inside material in Case 1 and Case 2 are shown in Fig. 2 and Fig. 3. And velocity inside material at 0.030 [s] is shown in Fig. 4.

Resin spread from center of material of high pressure to free surface of low pressure while pressing in each case. Since the friction between resin and plate is not considered, resin front was concave shape. But resin front is convex shape in actual phenomena because of the friction and solidification of resin around mold due to temperature difference inside material.

As time progressed, pressure rised at the bottom of resin firstly, and also rised at the top of resin as time progress. Then pressure rised in the center of resin, and finally, near free surface. Compared with the Case 1 and Case 2, pressure inside material droped and rised around fibers because of the effect of fibers. According to Fig. 4 which shows velocity inside material, fibers with high pressure flowed faster than resin. Rate of flow surface reached largest value near free surface and it decreased toward the center of material. Therefore, it is considered that fiber placement inside material has effects on fiber movement.

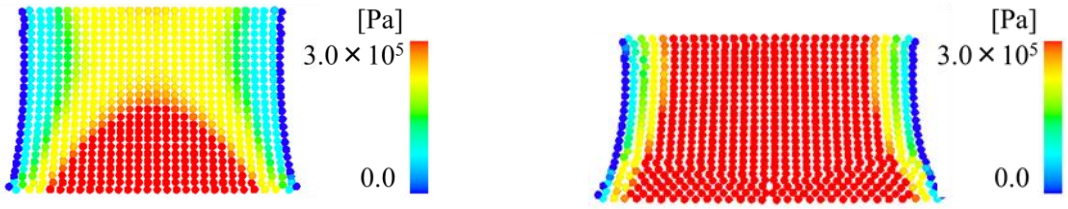

(a) 0.030 s (b) 0.043 s

Fig. 2 Analysis results of pressure distribution (Case 1).

Excerpt from ISBN 978-3-00-053387-7

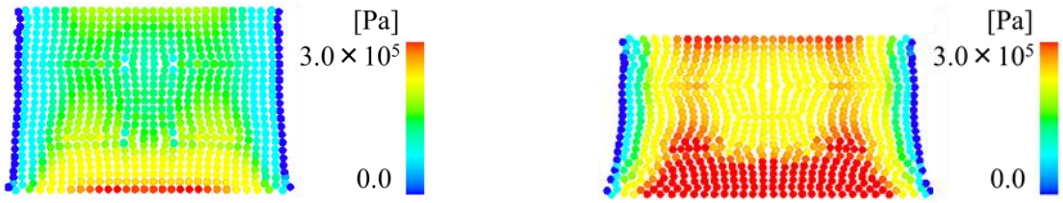

(a) 0.030 s (b) 0.043 s

Fig. 3 Analysis results of pressure distribution (Case 2).

(a) Case1 (b) Case2

Fig. 4 Analysis results of speed distribution at 0.030s.

3.2. Evaluation of the effect of fiber placement on fiber movement

The effect of initial fiber placement on fiber movement is evaluated. Analysis model is shown in Fig. 5. The parameter L which is distance between fibers in the upper of material is set different values such as 8, 10, 12, 14 mm and fibers and resin flowage is evaluated. Another analysis parameters are same as shown in section 3.1.

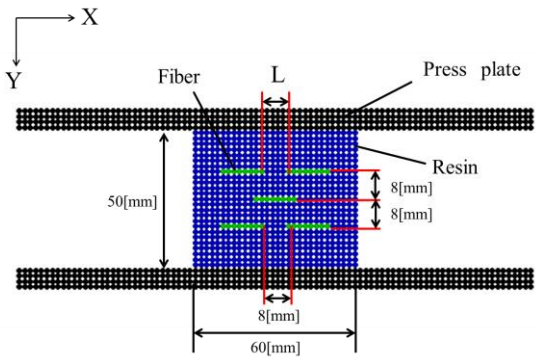

Fig. 5 Analysis model (Initial placement change of fiber).

The movement of fiber which was initially set in the upper right of resin in the X and Y - axis direction at 0.045[s] is shown in Fig. 6. There were small difference in each fiber movement for Y-axis direction. However there were large difference in X-axis direction. Fiber which was set near free surface initially reached largest value, and it decreased toward the center of resin. Therefore, it was suggested that initial fiber placement have effects on fiber movement.

Excerpt from ISBN 978-3-00-053387-7

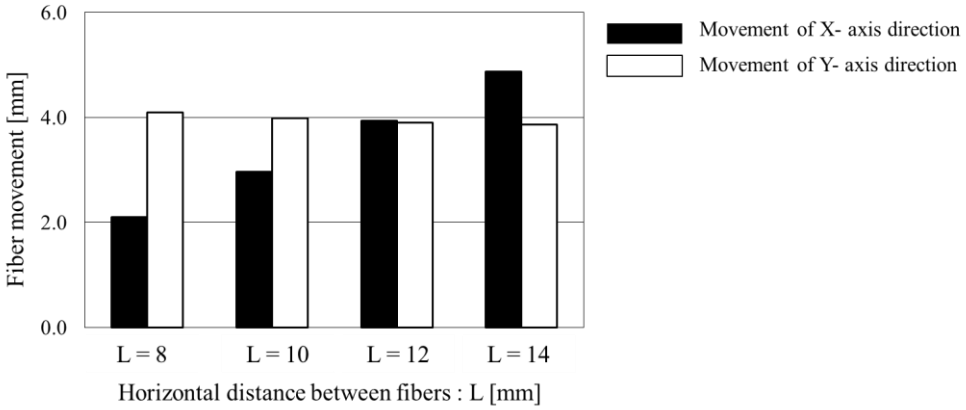

Fig.6 The movement of fiber which was in the upper right of resin at 0.045 s.

3.3. Analysis of 50 fibers in resin model in press forming

50 fibers and resin model is applied to during press forming analysis. Analysis model is shown in Fig. 7. The particle size is 1[mm], fiber length is 4[mm], the width of resin is 60[mm] and the height of material is 50[mm]. Time step is 1.0×10^{-4} [s] and the gravity is also considered as an external force. Analysis condition is summerized in Table 2.

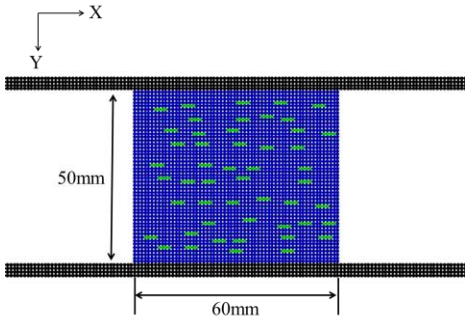

Fig. 7 Analysis model (Resin and 50 Fibers).

Table 2. parameter of 50 fibers and resin model.

Press acceleration α_p	12.0 [m/s^2]
Gravity acceleration g	9.8 [m/s^2]
Resin viscosity μ	1.0 [Pa・s]
Time step Δt	1.0×10^{-4} [s]

Resin and fibers flowage and pressure inside material at 6.0×10^{-2} [s] are shown in Fig. 8. As the result of section 3.1, the pressure reached largest value around fibers. Compared to the result of Case 2 in section 3.1 which is same size model, pressure inside material reached small value because fibers are distributed. Fibers which were set near free surface came out from the resin and the front shape of resin changes by fibers movement. And the accumulation of fibers were shown inside material.

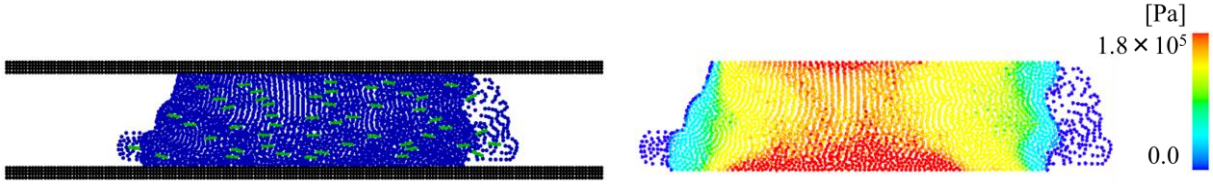

(a) Analysis result of resin and fiber flowage (b) Analysis result of pressure distribution

Fig. 8 Analysis result of pressure distribution at 0.06 [s].

Excerpt from ISBN 978-3-00-053387-7

Conclusion

The flowability of resin and fibers during press forming is analysed by using MPS method. In this study, to evaluate flowability of fiber and resin, following computational algorithms were implemented; 1) changing the calculation of viscosity term based on implicit method 2) Calculating flow of fiber as a rigid body. These algorithms allow flow calculation of high viscous fluid and shortening of calculation time in press forming.

Some analysis models are prepared for press forming. As a result, fibers dispersed pressure inside material, pressure rised around fibers, and fibers flowed faster than resin. Moreover, the velosity of fiber flow reached largest value near free surface, and it decreased toward the center of resin. Finally, fiber movement changed front shape of resin and accumulation of fibers were observed during press forming.

Therefore, it was suggested that the proposed numerical method was applicable to simulating press forming process of short fiber-reinforced composites.

References

[1] KEY WORLD ENERGY STATISTICS 2009
http://large.stanford.edu/courses/2009/ph204/landau1/docs/key_stats_2009.pdf

[2] H.Matsutani, I.Takeda, M.Hashimoto, N.Hirano, T.Okabe, Flow simulation of thermoplastic stampable sheet using particle method, *Journal of the Japan Society for Composite Materials*, 40, 5, 227-237, 2014

[3] K.Kawasaki, K.Ogiso, Sophistication of Two-Dimensional Multiphase Flow Model Taking into Account Lagrange Analysis of Rigid Bodies and Constitutive Law of Bingham fluid, *proceedings of coastal engineering* of *Japan Society of Civil Engineers*, vol. 55, p.36-40, 2008

[4] T.Okabe, H. Matsunami, T.Honda, S.Yashiro, "Numerical simulation of microscopic flow in a fiber bundle using the moving particle semi implicit method", Composites Part A, 43 (2012), 1765-1774

[5] S.Yahiro, H.Sakaki, T.Sakaida,Particle simulation for predicting fiber motion in injection molding of short-fiber-reinforced composites, *Composites:Part A*, 43, 1754-1764, 2012

[6] Y.Fukuzawa, H.Tomiyama, K.Shibata, S.Koshizuka, Numerical analysis of high viscous non-Newtonian fluid flow using the MPS method, *Transactions of Japan Society of Civil Engineers*, Paper No.20140007

Excerpt from ISBN 978-3-00-053387-7